Diffuse Reflectance FTIR Study of the Interaction of Alumina Surfaces with Ozone and Water Vapor

John M. Roscoe*

Department of Chemistry, Acadia University, Wolfville, NS, Canada B4P 2R6

Jonathan P. D. Abbatt

Department of Chemistry, University of Toronto, 80 St. George St., Toronto, ON, Canada M5S 3H6

Received: February 13, 2005; In Final Form: August 11, 2005

The interaction of ozone with alumina has been examined at ambient temperature as a function of ozone concentration and relative humidity. The experiments used diffuse reflectance FTIR spectroscopy in a small flow reactor, which provided control of the temperature, pressure, and composition of the gas mixture to which the sample was continuously exposed. Treatment of alumina with ozone produced a new spectroscopic feature at 1380 cm^{-1}, which we attribute to an aluminum oxide species formed by interaction of O_3 with Lewis acid sites on the alumina surface. After exposure of the alumina sample to O_3 was stopped, subsequent exposure of the sample to humidified nitrogen resulted in the slow removal of the peak at 1380 cm^{-1}. Simultaneously, the uptake of water by the alumina increased as indicated by the growth of the adsorbed water features which extend from approximately 3700 to 2500 cm^{-1}. Treatment of dry alumina with humidified ozone strongly inhibited both the rate of formation of the spectral feature at 1380 cm^{-1} and its limiting extent of formation. These observations are analyzed in terms of the adsorption and surface reaction properties of ozone on alumina. The observation that the new oxide feature on alumina, produced by reaction with ozone, can be removed by water is important for assessing the ability of mineral dust aerosols to process atmospheric trace gases over a significant time scale. We believe the work reported here to be the first direct and quantitative kinetic study of the competition between O_3 and water for adsorption sites on alumina.

Introduction

The environmental importance of atmospheric loading by solid aerosols is well-known and excellent reviews of the related chemistry and physics are available.[1−4] By far the dominant source of mineral dust aerosol is surface soil, which is raised by the winds and, in the case of the smaller size range of particles, can be transported over distances of several thousand kilometers. The composition of these mineral dust aerosols therefore mirrors the chemical composition of the Earth's crust, which is dominated by oxides of silicon and aluminum.

The transport of the smaller size fraction of mineral dust, with diameters less than a few tens of microns, over large distances raises the possibility that these materials might make an important contribution to the processing of atmospheric gases. The presence of comparatively strong Lewis acid sites on alumina[5−7] leads to the adsorption of Lewis bases such as water and ozone. The adsorption of these substances on alumina has been characterized[5−7] and recent kinetics work in our laboratory[8] and others[9−12] has indicated that uptake of ozone on alumina leads to destruction of ozone with the accompanying passivation of the alumina surface. Although some recovery of the surface activity was observed in the absence of ozone, the recovery of the surface activity was slow, incomplete, and variable. These experiments monitored the loss of gas phase ozone directly in a static system and uptake coefficients for ozone on alumina were calculated from these measurements. The results were interpreted to indicate some catalytic activity for ozone destruction with partial regeneration of the active sites during an experiment (see also refs 9 and 10).

We report here experiments, made under flow conditions, which examine changes in the surface of powdered alumina as a result of heterogeneous ozone destruction. These experiments are distinct from those noted above which were obtained in a static system and measured the loss of ozone from the gas phase in the presence of an alumina deposit. The results we now report permit direct observation of changes produced on the alumina surface, as a result of exposure to ozone, using diffuse reflectance Fourier transform infrared spectroscopy (DRIFTS). These experiments permit direct observation of the kinetics of changes in the concentrations of species on the alumina surface in response to changes in the composition of the flowing gas. Consequently, we are able to observe the changes in the alumina surface which coincide with both its passivation and reactivation toward destruction of ozone. We are also able to examine the response to variations in relative humidity of alumina surface features related to the uptake of ozone. These experiments provide information on the way in which variation in relative humidity is likely to influence the mechanism by which ozone is processed by an atmospheric aerosol containing a mineral such as alumina which presents Lewis acid sites.

Experimental Section

A schematic diagram of the flow cell and gas handling system is provided in Figure 1. The heart of the system is the DRIFTS flow cell, which was made by replacing the base of a Harrick

* To whom correspondence should be addressed. E-mail: john.roscoe@acadiau.ca.

10.1021/jp050766r CCC: $30.25
Published on Web 09/13/2005

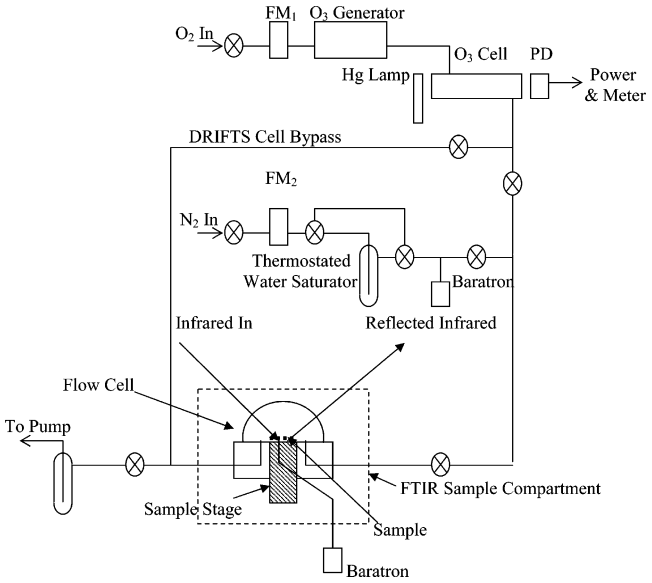

Figure 1. Schematic diagram of the DRIFTS cell and gas handling system. FM_1 and FM_2 are mass flowmeters and PD is a photodiode detector.

DRP-NI6 DRIFTS cell with one of identical dimensions but made of Teflon and fitted with a Teflon coated copper sample stage. Three lines were provided for connection to a vacuum pump, a Baratron pressure gauge, and a line for admitting the gas mixture of interest. The sample stage could be removed for cleaning. While the experiments reported here were all done at ambient temperature, the sample stage could be heated or cooled as desired and a thermocouple inserted close to the end adjacent to the sample permitted monitoring the sample temperature. All connections to the sample holder were made of stainless steel and the connections to the gas handling system were made of Teflon tubing. The dome on the sample holder had a diameter of 3 cm and its volume was approximately 7 cm^3. The dome was sealed to the base with an O-ring and had three windows, one of which was used for visual observation while the other two were made of zinc selenide and permitted entry and exit of the infrared beam and the diffusely scattered infrared light, respectively. The entire DRIFTS flow cell was enclosed in the mounting assembly supplied by the manufacturer of the original DRIFTS cell. This mounting assembly contained the complete praying mantis optical assembly for the DRIFTS experiments and was purged with dry, CO_2 free nitrogen. It was mounted in the sample compartment of a Nicolet Magna 550 Series 2 FTIR spectrometer.

The gas handling system was constructed from stainless steel fittings, Teflon tubing, and Pyrex traps and photometric measurement cells. Flow rates of O_2 and N_2 were measured with MKS model 247C mass flowmeters. Pressures were measured with MKS Baratron capacitance pressure gauges. Ozone was produced photochemically in a stream of O_2 with a Jelight model 1000 ozone generator. The O_3 concentration in the gas stream emerging from the ozone generator was determined by measuring its absorbance in a Pyrex absorption cell with an optical path length of 10.1 cm using a mercury pen ray lamp and a photodiode. A bypass line permitted the O_3 stream to be directed around the DRIFTS cell while the experimental conditions stabilized after which it could be redirected into the DRIFTS cell at the desired time. The water content of the gas mixture entering the DRIFTS cell was controlled by passing a suitable flow rate of N_2 through a coarse glass frit in a trap containing deionized water. The vapor pressure of the water in the trap was controlled by a constant-temperature bath and the partial pressure of water in the gas stream was calculated from the known temperature and tabulated values of the vapor pressure of water as a function of temperature. The total pressure in the line used to control addition of water to the reaction vessel was measured with a Baratron pressure gauge.

Alumina powder (Aldrich, 99.7%, $<10\ \mu m$) was taken from the same sample used in the earlier work from this laboratory.[8] It was deposited on the sample stage in the DRIFTS cell by preparing a slurry of approximately 50 to 100 mg of alumina in 10 to 12 drops of ethanol, 2 to 3 drops of which were deposited on the sample stage with a Pasteur pipet. This deposit was allowed to air-dry for 10 to 15 min after which it was evacuated for at least 1 h until the base pressure of the system was reached and the DRIFTS spectrum of the deposit showed no change on further evacuation. The mass of alumina deposited in this way was determined by difference for each experiment and ranged from approximately 2 to 20 mg, with most experiments using a deposit of between about 8 and 12 mg. This procedure produced a circular pellet with a diameter of approximately 0.9 cm, which appeared visually to be of uniform thickness. The thickness of these pellets was approximately 10 times that of the alumina films used in the earlier experiments from this laboratory.[8] DRIFTS spectra were usually obtained at a resolution of 4 cm^{-1} averaged over 1000 interferometer scans. The spectra were baseline corrected and the required peaks were then integrated digitally over the desired range of wavenumbers. The times used in the kinetic analysis were those at which the spectrum scan was started. It may be shown that, for first-order kinetics, the time corresponding to the average of a constant number of interferometer scans differs by a constant amount from the time at which the spectrum scan is started.

Results

Treatment of alumina with dry O_3 produced peaks in the infrared reflectance spectrum at 1740 and 1380 cm^{-1} which we attribute to formation of new oxide species on the alumina surface. Unfortunately, the reflectance of the alumina was too small below approximately 1100 cm^{-1} to provide useful spectra and this prevented us from obtaining spectra in the region below 1000 cm^{-1} in which spectral features attributable to peroxide species are expected to occur.[13] The peak at 1380 cm^{-1} was by far the stronger of these new peaks and was used to evaluate the change in the alumina surface on exposure to O_3. It also occurred in a region in which interference from adsorbed and gas-phase water was minimal. Spectra of adsorbed and gas-phase water as well as that of the ozone treated alumina are presented, offset from each other for convenience, in Figure 2. The DRIFTS sample stage was not sufficiently reflective to provide a good quality spectrum of gas-phase water in the absence of alumina. For that reason, the gas-phase water spectrum presented in Figure 2 was obtained in a conventional gas cell using the same resolution as in the measurements with the DRIFTS experiments and the absorbance was scaled to be consistent with the DRIFTS spectra presented in that figure. Vertical lines indicate the range of wavenumbers over which the peaks for adsorbed water and for the new aluminum oxide species were integrated. While the 1740 cm^{-1} peak was completely obscured by absorption due to gas-phase water, the area of the 1380 cm^{-1} peak could be measured in the indicated wavenumber range with minimal interference from gas phase water. Although the inability to obtain a reference spectrum of good quality for gas phase water prevented us from making

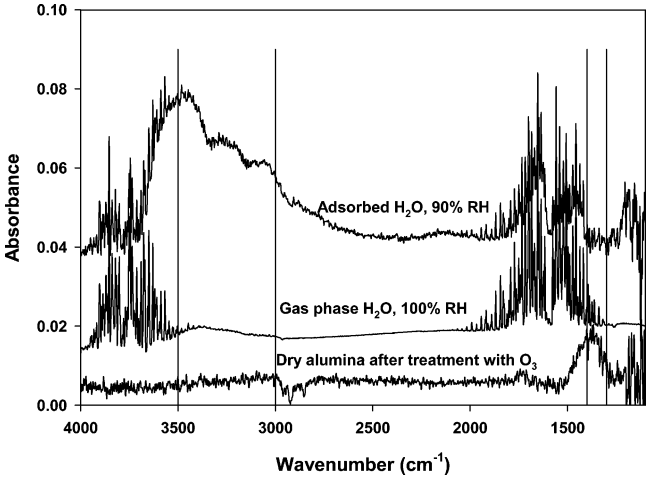

Figure 2. FTIR spectra of gas-phase water, water adsorbed on alumina, and dry alumina after treatment with O_3. The spectra are offset vertically for convenience. The vertical lines indicate the limits used to integrate the peaks attributed to adsorbed water (3500 to 3000 cm^{-1}) and to the newly formed oxide (1400 to 1300 cm^{-1}).

corrections for background due to gas phase water by subtracting its contribution to the area of the oxide peak, absorbance due to gas phase water could be adequately compensated by making a small baseline correction using the "tangent skim" approach with the measured spectra. At most of the lower relative humidities examined, the baseline before the 1380 cm^{-1} peak was the same as that after the peak, within measuring uncertainty, suggesting that interference from gas phase water was not important under those conditions. At even the larger relative humidities these baseline corrections were small. Absorbance due to adsorbed water is clearly visible in the region between 3700 and 2500 cm^{-1} and the spectral range from 3500 to 3000 cm^{-1}, which was used for monitoring the amount of adsorbed water, is clearly free of interference from gas-phase water. Integration was not extended below 3000 cm^{-1} because of the presence of a small negative feature at roughly 2900 cm^{-1}, which often appeared on treatment with ozone. This could be attributable to the presence in the alumina sample of a small amount of adventitious organic matter that was removed by the ozone.

The rate of growth of the peak at 1380 cm^{-1} for three samples of different masses exposed to differing concentrations of O_3 and water vapor is indicated in Figure 3. Growth of the peak at 1380 cm^{-1} followed first-order kinetics and the curves in Figure 3 are standard first-order growth curves fitted to the experimental data. Figures 4 and 5 present the response of the pseudo-first-order rate constants, calculated from first-order kinetic analysis of the integrated areas of the 1380 cm^{-1} peak, to variations in O_3 concentration and relative humidity of the flowing gas. Two features are immediately evident from the results of Figures 3 through 5. In the absence of water, the kinetics of the growth of the newly formed oxide and its maximum extent of production do not depend strongly on the ozone concentration. The alumina deposits used for the results in this figure cover a mass range of 8 to 14 mg, which implies a sample thickness of approximately 50 μm. The alumina sample used to prepare the deposits had a grain size of less than 10 μm so our samples are relatively thick. The DRIFTS technique samples only the top few layers of the deposit so, although the precise area sampled is not well defined, it is reasonable to conclude that the effective surface area sampled by the DRIFTS measurement is similar from sample to sample. The lack of dependence on O_3 concentration at all but the smallest measurable concentrations

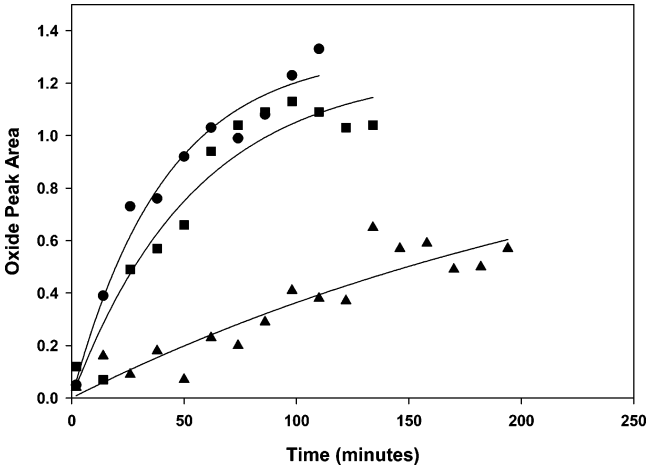

Figure 3. Growth of the FTIR peak at 1380 cm^{-1}, measured by integrating the peak from 1400 to 1300 cm^{-1}, on treatment of alumina with dry and humidified ozone: (●) dry O_2, 13.0 mg of Al_2O_3, $[O_3] = 2.5 \times 10^{13}$ molecules cm^{-3}, (■) equal amounts of dry N_2 and O_2, 14.1 mg of Al_2O_3, $[O_3] = 1.3 \times 10^{13}$ molecules cm^{-3}, (▲) equal amounts of dry O_2 and humidified N_2, 13% relative humidity, 8.0 mg of Al_2O_3, $[O_3] = 2.0 \times 10^{13}$ molecules cm^{-3}. The lines are first-order growth curves fitted to the individual data sets using the function $y = a(1 - e^{-kt})$.

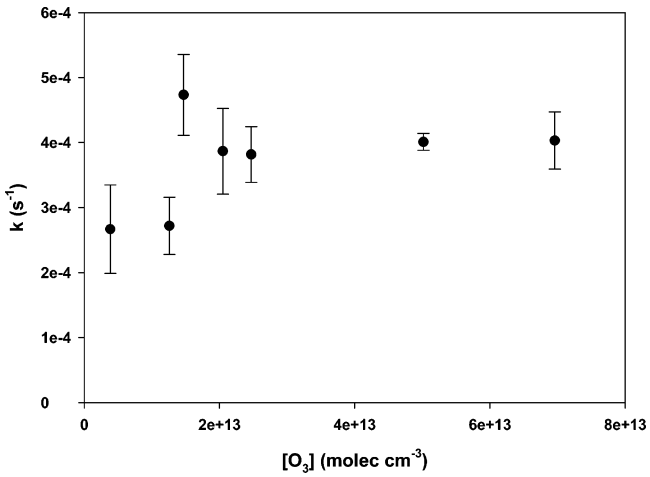

Figure 4. Dependence on ozone concentration of the pseudo-first-order rate constant for oxide growth on dry alumina. Error bars indicate one standard deviation.

would be consistent with rapid saturation of the alumina surface with O_3 followed by slower production of the oxide species responsible for the spectroscopic feature observed at 1380 cm^{-1}. While the growth of the peak at 1380 cm^{-1} follows pseudo-first-order behavior, as a result of maintaining a constant ozone concentration during a given experiment, the form of the dependence on ozone concentration of the pseudo-first-order rate constant for production of the new oxide is not clear. The lower limit of our sensitivity for measuring the concentration of O_3 prevented us from measuring these rate constants at lower O_3 concentrations. However, in the absence of O_3 the peak at 1380 cm^{-1} was not observed and this, together with the observation of a nearly constant pseudo-first-order rate constant for production of the new oxide under most of the accessible O_3 concentrations in our apparatus, suggests a complex dependence on O_3. Such a dependence would require a rapid increase from zero in the pseudo-first-order rate constant at very small concentrations of O_3 below our measurement capability, reaching a nearly constant value over most of the range of O_3 concentrations which we could measure.

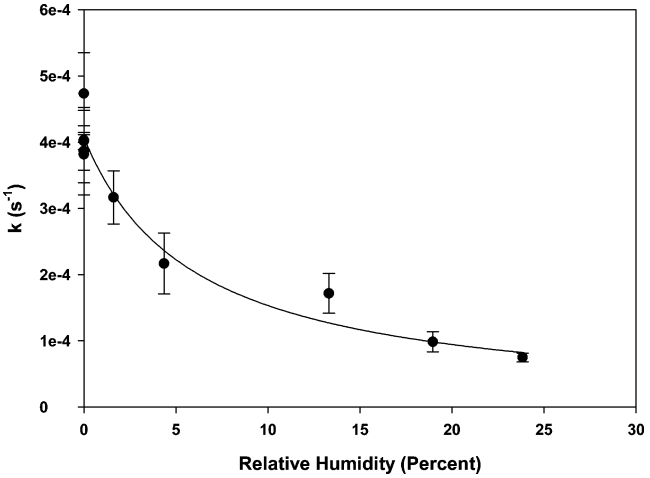

Figure 5. Dependence on relative humidity of the pseudo-first-order rate constant for oxide growth on alumina. O_3 concentrations were sufficiently large to ensure that there was no dependence on the concentration of O_3. The curve is an exponential function and is intended only to guide the reader's eye. Error bars indicate one standard deviation.

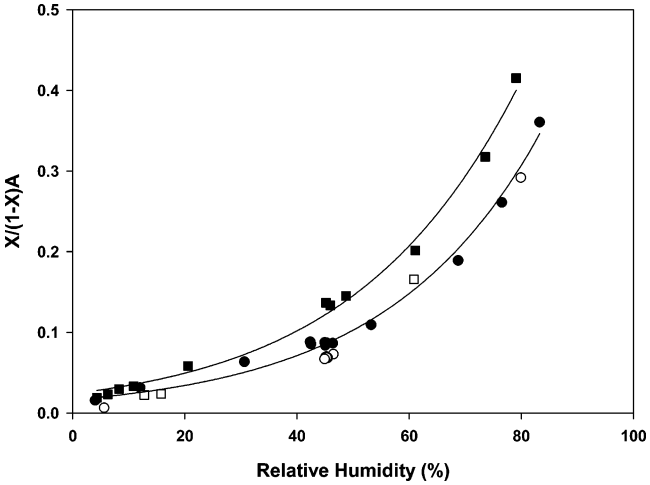

Figure 6. Adsorption of water on alumina before and after treatment with ozone, presented in BET format. In this figure, X is percent relative humidity and A is the absorbance integrated between 3500 and 3000 cm^{-1} in the DRIFTS spectrum. (●) Increasing relative humidity before ozone treatment, (○) decreasing relative humidity before ozone treatment, (■) increasing relative humidity after ozone treatment, (□) decreasing relative humidity after ozone treatment. The curves are exponential functions and are intended only to guide the reader's eye.

It is clear from Figures 3 and 5 that use of humidified ozone has a dramatic effect on both the rate of formation of the new oxide, represented by the peak at 1380 cm^{-1}, and its maximum extent of formation. In the experiments represented in Figure 5, the O_3 concentrations were sufficiently large to fall well within the range over which the pseudo-first-order rate constants were effectively independent of the O_3 concentration as indicated in Figure 4. Most of the O_3 concentrations used in the experiments of Figure 5 were between 1.7×10^{13} and 2.5×10^{13} molecules cm^{-3}. Several experiments were made in which the O_3 cell of Figure 1 was moved from the inlet to the outlet of the DRIFTS cell in an effort to assess the effect of the alumina deposit on the ozone concentration in the gas phase. In these experiments, the O_3 concentration was monitored as a function of time following its introduction to the DRIFTS cell containing a typical quantity of dry alumina. In all cases, the O_3 concentration increased within approximately 1 min to values that were comparable to the measured inlet concentrations in the other experiments made with comparable flow rates of O_2 in the ozone generator. We conclude from this result that the measured O_3 concentration at the inlet of the DRIFTS cell is representative of the actual O_3 concentration inside the DRIFTS cell and that the changes in the FTIR spectra are a result of changes that occur in the presence of the constant measured inlet O_3 concentrations. The results in Figure 5 suggest that the production of the new oxide slows dramatically in the presence of water, reaching a small and possibly constant nonzero value at roughly 20% relative humidity. However, it is not clear from these experiments whether the water is simply competing with O_3 for the Lewis acid sites on the alumina or if the water is able to remove some of the newly formed oxide.

Adsorption of water on alumina showed qualitatively the same behavior as that measured in a recent more detailed study.[7] This is illustrated in Figure 6 in which the adsorption isotherm for water on alumina, plotted in the conventional BET format, is shown before and after treatment of the alumina sample with ozone. This BET function, reproduced below, differs from that used in ref 7 only in the use of absorbance in place of the volume

$$\frac{X}{(1-X)A} = \frac{1}{A_m c} + \frac{(c-1)}{A_m c}X; \qquad X = \frac{P}{P_0}$$

of water adsorbed. The volume of water adsorbed was assumed to be proportional to the area in the DRIFTS spectra integrated between 3500 and 3000 cm^{-1}. In this equation, P_0 is the saturation vapor pressure of water at the temperature of the experiment, P is the partial pressure of water vapor producing an absorbance A due to adsorbed water, c is the BET adsorption coefficient, and A_m is the absorbance due to adsorbed water under monolayer coverage conditions. Before the ozone treatment, the isotherm showed no discernible hysteresis with data points obtained on increasing the relative humidity merging smoothly with those obtained on decreasing the relative humidity. However, after treatment with ozone the data points in Figure 6 obtained by systematically increasing the relative humidity lie consistently above those obtained with the same alumina sample before the ozone treatment. This indicates that the sample treated with ozone was less able to adsorb water than it had been before the ozone treatment. When the relative humidity was then systematically decreased, Figure 6 indicates that the data points fell close to those obtained before the ozone treatment. We interpret this behavior as indicating that the ozone treatment produces a surface species that occupies Lewis acid sites which would normally be available to water and that exposure to water removes the surface species occupying these sites allowing the water to once again be adsorbed on them. We therefore made a series of simultaneous measurements of the rate of water uptake and loss of the oxide as measured by the area of the peak at 1380 cm^{-1} to obtain further information about the relationship between loss of the newly formed surface oxide and the concomitant increase in water adsorption.

Figure 7 indicates the temporal evolution of adsorbed water and the new oxide represented by the peak at 1380 cm^{-1} in a typical experiment in which an alumina sample was first exposed to dry ozone until nearly the maximum amount of the new oxide was formed. The oxidized sample was then exposed to a mixture of dry oxygen and dry nitrogen for a period of time, and the oxidized sample was then exposed to humidified nitrogen producing a constant, known relative humidity in the DRIFTS cell. It is clear that the newly formed oxide remains stable in the presence of dry N_2 and dry O_2. Indeed, experiments in which an oxidized sample was exposed to flowing dry nitrogen

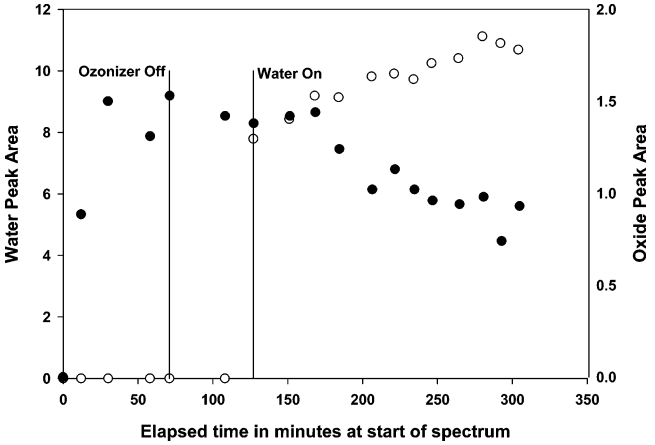

Figure 7. Simultaneous evolution of the oxide peak at 1380 cm^{-1} and adsorbed water on treatment of alumina with dry ozone followed by treatment of the oxidized sample with humidified nitrogen. In the time period between turning the ozonizer off and adding water, the sample was exposed to a mixture of dry O_2 and dry N_2. During the water exposure, the relative humidity in the DRIFTS cell was 77%. The peaks were integrated between the limits identified in Figure 2. (○) Adsorbed water area integrated from 3500 to 3000 cm^{-1}. (●) Area of the oxide feature at 1380 cm^{-1}.

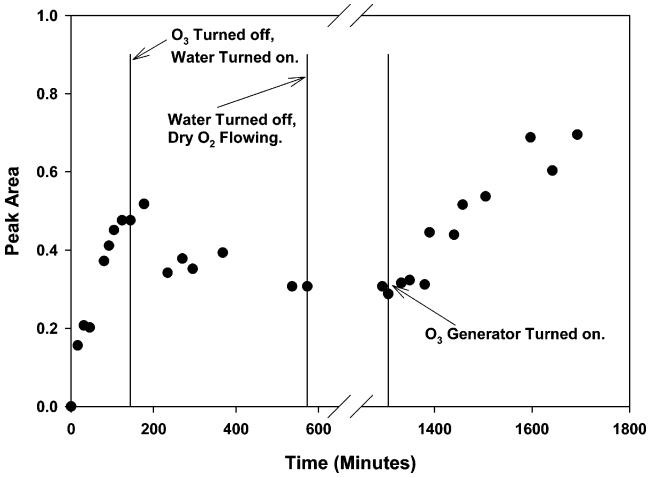

Figure 8. Production of the FTIR peak at 1380 cm^{-1} on dry alumina using dry O_3 at a concentration of 1.2×10^{14} molecules cm^{-3}, its partial removal at 35% relative humidity in a stream of humidified nitrogen, and the subsequent regeneration of this feature in dry O_3 at a concentration of 4.7×10^{13} molecules cm^{-3} after purging with a stream of dry O_2 for several hours to remove adsorbed water. Peak areas were integrated between 1400 and 1300 cm^{-1} as indicated in Figure 2.

overnight showed no measurable loss of the peak at 1380 cm^{-1}. However, on raising the relative humidity in the DRIFTS cell, the peak at 1380 cm^{-1} slowly disappeared while the amount of adsorbed water slowly increased. The rate of change of both the oxide and the adsorbed water increased with increasing relative humidity.

Both the loss of oxide and the increase in water adsorption followed first-order kinetics. Complete removal of the peak at 1380 cm^{-1} was never observed on the time scale available for the experiments, although at high relative humidity this peak ultimately became very small. The increase in area of the peaks between 3500 and 3000 cm^{-1} due to adsorbed water always reached a well-defined limiting value. While the slowness of the changes produced by exposure of the newly formed oxide to water vapor seriously detracted from our ability to calculate precise pseudo-first-order rate constants, it was clear that for both the removal of oxide and the increased water uptake the pseudo-first-order rate constants increased with increasing relative humidity, reaching a limiting value above roughly 40% relative humidity. The rate constants for increased water uptake are generally about a factor of 3 to 4 larger than those for oxide loss at a given value of relative humidity.

The results presented so far demonstrate that treatment of alumina with O_3 produces a new surface oxide that is stable under dry conditions but is removed by treatment with humidified nitrogen. It is also clear that removal of this surface oxide is accompanied by increased uptake of water. It remains to be determined if these freshly regenerated Lewis acid sites which are able to adsorb additional water are also capable of producing the oxide responsible for the FTIR peak at 1380 cm^{-1} on renewed treatment with O_3 or if the additional water that has adsorbed on these sites blocks them to reaction with O_3. Figure 8 presents the results of an experiment intended to answer this question. A fresh, dry alumina deposit was exposed to flowing O_3 at a constant ozone concentration of 1.2×10^{14} molecules cm^{-3} until the FTIR peak at 1380 cm^{-1} was well developed. At this point, the ozone generator was turned off and the oxygen stream was replaced by a stream of humidified nitrogen, exposing the sample to a relative humidity of 35%. This produced a slow removal of the peak at 1380 cm^{-1}. As anticipated from the kinetic measurements of loss of this peak on exposure to water, the slowness of this process made it impractical to attempt complete removal of the newly formed oxide. After the peak at 1380 cm^{-1} had decreased significantly, the nitrogen stream was replaced by the oxygen stream from the ozone generator and the sample was exposed to a stream of dry O_2 for several hours to remove adsorbed water vapor since it is clear from the previous experiments that adsorbed water inhibits formation of the new oxide on exposure to ozone. Finally, the ozone generator was turned on again and the growth of the FTIR peak at 1380 cm^{-1} was monitored. It is clear that, after a short warm up period during which the ozone generator establishes a steady flow of O_3, the FTIR peak at 1380 cm^{-1} grows back to a signal which is comparable to that measured before the treatment with water vapor. The average O_3 concentration in this part of the experiment was 4.7×10^{13} molecules cm^{-3}. Continued exposure to O_3 continued to oxidize Lewis acid sites that had not been processed during the initial, incomplete, oxidation with O_3.

Discussion

Treatment of Alumina with O_3 in the Absence of Water Vapor. It is known from work both in our laboratory[8] and by others[1] that gas-phase ozone is lost upon exposure to alumina surfaces. It is reasonable to assume that the appearance of the oxide, represented by the FTIR peak at 1380 cm^{-1}, on the alumina surface is coincident with this ozone loss. In particular, in our laboratory[8] it was previously observed in a static system that the initial destruction of ozone is rapid, with a half-life on the order of tens of seconds. However, it was also observed that the destruction of ozone continued during multiple dosings of ozone to the alumina surface, albeit at significantly slower rates. In the work presented here, because we are unable to spectroscopically observe the alumina surface after only very small ozone exposure, we believe that we are observing the kinetics that occur on partially deactivated alumina films. This is consistent with the appearance of the new aluminum oxide peak in the FTIR spectra with a relatively slow half-life of the order of tens of minutes.

The FTIR spectra produced when mineral oxides are exposed to O_3 have received previous attention.[5,6] The results obtained with titania and alumina are particularly relevant to the present

work because both these oxides present strong Lewis acid sites with those on alumina being the stronger. Strong Lewis acid sites were found to efficiently decompose O_3 by dissociative adsorption. In the case of alumina,[6] no spectral features were found that could be attributed to adsorbed O_3 suggesting that the O_3 decomposed immediately on adsorption and SCF calculations indicated that this decomposition produced O_2 and an atom of $O(^1D)$, which remained bound to a Lewis acid site. It was proposed[5] that these $O(^1D)$ atoms can then participate in catalytic removal of O_3. While these spectra were obtained primarily at liquid nitrogen temperature, the general conclusions are likely to also be applicable in our experiments at ambient temperature. The reported spectra do not, however, cover the wavenumber range in which we observe the peak at 1380 cm^{-1}.

The vibrational frequencies of oxygen species bound to metal surfaces have been summarized by Che and Tench.[13] M−O species generally absorb in the 800−1000 cm^{-1} region while M═O species absorb from about 900 to 1100 cm^{-1}. This reflects the effect of increasing bond strength. "Neutral O_2" is cited as absorbing over the broad range 1460−1700 cm^{-1} and the authors discuss the significant role of π back-bonding contributing to the strength of bonding of O_2 to the metal surface and thereby influencing the vibrational frequency. The peak which we observe at 1380 cm^{-1} could be due to a particularly strong M═O bond due to the $O(^1D)$ atom attached to a strong Lewis acid site on the alumina surface as proposed by Thomas et al.[6] The comparatively large Lewis acid strength of these sites on alumina would be expected to result in relatively strong M═O bonds, shifting the absorption to significantly larger wavenumbers than are observed on other metal oxides.[5,6,13] On the other hand, the position of this peak could also be consistent with the "neutral O_2" adsorbed species discussed by Che and Tench.[13] Both $O(^1D)$ and O_2 are expected as reaction products of the decomposition of O_3 on alumina so either interpretation would be consistent with this peak at 1380 cm^{-1} being due to oxidation of the alumina surface by O_3. The comparative stability of the FTIR peak at 1380 cm^{-1} to long-term exposure to flowing nitrogen and to evacuation suggests that it is more likely to be due to a M═O species. This is also consistent with the identification of a peak at 1345 cm^{-1} as being due to Al═O in experiments in which aluminum metal was subjected to plasma oxidation.[14] However, definitive assignment of the 1380 cm^{-1} band observed in our experiments to a specific chemical species and vibrational mode would require a much more exhaustive spectroscopic examination than was possible in our work.

The relatively slow development of the peak at 1380 cm^{-1} and the accompanying decrease in the ability of the alumina to adsorb water suggests that this new spectroscopic feature represents a surface oxide species that inhibits both the adsorption of water and destruction of ozone by binding to Lewis acid sites which would otherwise be available for adsorption of water and possibly also for interaction with ozone. This may be represented by the following sequence of reactions in which "s" is a surface site, sO_3 is an adsorbed ozone molecule, and sO and sO_2 are two different surface oxide species.

$$O_3 + s \rightarrow sO_3 \quad (1)$$

$$sO_3 \rightarrow sO + O_2 \quad (2)$$

$$sO + O_3 \rightarrow sO_2 + O_2 \quad (3)$$

This is a simple modification of a mechanism proposed by Li et al.[15,16] in which we have separated their first reaction into reaction steps 1 and 2 and have omitted, for the moment, their third step in which the sO_2 species decomposes, regenerating the surface site and liberating O_2. If reactions 1 and 2 are fast, the rapid uptake of O_3 would be explained. Reaction 3 would then permit up to two O_3 molecules to be removed for every available Lewis acid site. This would be consistent with the conclusion from earlier experiments[8,9] that destruction of ozone on alumina is catalytic to a degree. The occurrence of reaction 3 would also result in gradual passivation of the alumina surface, assuming sO_2 to be a stable species, and would be consistent with the decrease in reactivity toward O_3 found in earlier experiments.[8] Additional catalytic activity, as well as some additional control over the rate of passivation, would result by introduction of reactions such as

$$sO_2 \rightarrow s + O_2 \quad (4)$$

as suggested by Li et al.[15,16] or

$$2sO \rightarrow 2s + O_2 \quad (5)$$

as suggested by Sullivan et al.,[8] both of which regenerate active surface sites. The presumption is that the new FTIR peak at 1380 cm^{-1} observed in our experiments on treatment of the alumina samples with O_3 is attributable to a surface oxide species that is taken to represent a final oxidation product resulting from the ozone treatment. This stable surface oxide would then tie up surface sites which would otherwise be able to process ozone, leading to gradual inhibition of ozone loss.

It is fruitful to compare the operating conditions in this work to those used in our previous study in a static chamber.[8] In particular, the alumina was taken from the same commercial source and presumably had the same specific surface area and intrinsic chemical activity. Ozone concentrations were also overlapping, i.e., typically 2×10^{13} molecules cm^{-3} in our experiments and values of 4×10^{13} molecules cm^{-3} used in experiments in our earlier work, such as those presented in Figure 4 in ref 8. Under the assumption that the full mass of substrate is available for reaction, total surface areas were also comparable, typically about 200 cm^2 in our experiments and about 100 cm^2 in the experiments of their Figure 4.[8] Taking into account the different reaction volumes (408 cm^3 in ref 8 compared to our volume of 7 cm^3) and for comparable uptake coefficients the first-order rate constant for ozone loss in our system would be about a factor of 50 to 100 larger than the values obtained in the static experiments. This corresponds to a lifetime for initial ozone loss that is much shorter than the observation time of the FTIR, which is approximately 12 min as required by the number of scans that must be collected to measure a good spectrum. This supports our contention that the spectroscopic changes we observe in this work arise on a surface that is already partially oxidized and passivated. Indeed, we observed in this work that the concentration of ozone exiting the DRIFTS cell was fairly constant, after an initial exposure period of a minute or so. In the static experiments,[8] such conditions were attained by a few repeated dosings of ozone to the alumina films, at which point ozone had a long half-life.

The measurements of ozone concentrations at the exit of the DRIFTS cell immediately after diversion of the ozone flow into the cell, exposing it to a fresh alumina deposit, gave approximately first-order kinetics. The first-order rate constants calculated from these results led to uptake coefficients (γ) of approximately 1×10^{-7}, assuming that the alumina deposits are sufficiently thin that the ozone can access the entire alumina surface. This value is comparable to the values of 1.4×10^{-7} and 8.0×10^{-8} calculated from the overall ozone loss, rather

than the initial uptake, in the third and fourth oxidations represented in Figure 4 of the results from the static experiments.[8] Again, the similarity of these values of the ozone uptake coefficients supports our conclusion that the experiments in our DRIFTS cell were obtained under conditions that correspond to those in the static experiments that were made on partially passivated alumina films.

Treatment of Alumina with O_3 in the Presence of Water Vapor. The data of Figures 3 and 5 indicate that the first-order rate constant for production of the oxide peak at 1380 cm^{-1} decreases rapidly with increasing relative humidity. We also found that alumina samples that were not subjected to prolonged, rigorous evacuation before use to remove adsorbed water did not form the species responsible for the peak at 1380 cm^{-1}. The observed dramatic decrease in the rate of formation of the surface species giving rise to the new peak at 1380 cm^{-1} when alumina is treated with humidified O_3 suggests either that water adsorbs to a surface site that is required for production of the newly formed oxide or that water reacts sufficiently rapidly with the oxide that both its rate of formation and its ultimate extent of formation are reduced. The observation that the removal of oxide by water is slow, combined with the failure of the oxide to form on alumina surfaces that had not been rigorously dried, suggests that water adsorbs strongly to sites that would otherwise bind O_3, inhibiting formation of the oxide.

The adsorption of water before and after treatment of the alumina with O_3 provides further information about the nature of the sites on the alumina surface. As noted earlier, experiments with dry O_3 in a static system clearly demonstrated that ozone uptake is eventually largely suppressed, presumably by formation of a new, stable, surface species that blocks further adsorption. In contrast, treatment of the alumina with ozone produces a surface species that only partially blocks adsorption of water. Indeed, we see from the data in Figures 6 and 7 that treatment with O_3 blocks only about 30% of the surface sites on which water normally adsorbs at relative humidities at which water is able to produce saturation coverage of an untreated alumina surface.

Exposure of the alumina to water after treatment with O_3 results in two effects, indicated in Figure 7. Slow removal of the spectroscopic feature at 1380 cm^{-1} occurs accompanied by an increase in the extent of water adsorption indicated by the spectroscopic features between 3700 and 2500 cm^{-1}. This indicates a reaction between the surface oxide and water which regenerates surface sites that are capable of adsorbing water. This effect suggests that water is a sufficiently strong Lewis base that it is able to displace the surface oxide species that is responsible for the FTIR peak at 1380 cm^{-1}, thereby simultaneously decreasing the intensity of that peak and increasing the intensity of the peaks between 3000 and 3500 cm^{-1} which are due to adsorbed water. The observation that the first-order rate constant for water uptake is substantially larger than that for oxide loss suggests that water adsorbs as clusters. Such behavior would be consistent with other work on the adsorption of water on alumina and on mica[7,17,18] in which it was also concluded that water adsorbed on mica and alumina in clusters.

Atmospheric Implications

From an atmospheric perspective, it has been suggested that mineral dust may play a role in the destruction of tropospheric ozone, particularly in localized regions such as those downwind of the Sahara and Asia. While the initial uptake coefficients for ozone loss on dust are near the lower limit of being atmospherically relevant as an ozone loss mechanism, those on partially oxidized dust are not.[1,2,9−12,19−21] Using alumina as a model for metal oxides present in mineral dust, we have shown that exposure of an oxidized alumina deposit to water vapor removes the newly formed oxide and restores Lewis acid sites that had previously been capable of adsorbing water and of being oxidized by ozone. Regeneration of deactivated surface sites by exposure to water could result in enhanced efficiency of the alumina surface for processing O_3. Restoration of these reactive surface sites would lead to a much larger effective alumina surface area being active in ozone destruction than would be the case for dry conditions, i.e., catalytic behavior could be observed. We believe the experiments reported here to be the first direct and quantitative measurement of the competition between O_3 and water for Lewis acid sites on mineral dusts. The regeneration of Lewis acid sites on exposure to water vapor has the potential to restore the ability of mineral dust aerosols to process ozone, particularly at low relative humidities. The role of water vapor in mediation of the reactivity of mineral dusts deserves consideration in evaluating the long-term effects of such aerosols on atmospheric trace gases as they traverse long distances and encounter a wide range of relative humidities.

Acknowledgment. Financial support for this work was provided by the Natural Sciences and Engineering Research Council of Canada, Acadia University, and the Canada Foundation for Innovation.

References and Notes

(1) Usher, C. R.; Michel, A. E.; Grassian, V. H. *Chem. Rev.* **2003**, *103*, 4883.
(2) Al-Abadleh, H. A.; Grassian, V. H. *Surf. Sci. Rep.* **2003**, *52*, 63.
(3) Seinfeld, J. H.; Pandis, S. N. *Atmospheric Chemistry and Physics*; John Wiley & Sons: New York, 1997.
(4) Jonas, P. R.; Rodhe, H. *Climate Change 1994*; Houghton, J. T., Ed.; Cambridge University Press: New York, 1995.
(5) Bulanin, K. M.; Lavalley, J. C.; Tsyganenko, A. A. *Colloids Surf., A* **1995**, *101*, 153.
(6) Thomas, K.; Hoggan, P. E.; Mariey, L.; Lamotte, J.; Lavalley, J. C. *Catal. Lett.* **1997**, *46*, 77.
(7) Al-Abadleh, H. A.; Grassian, V. H. *Langmuir* **2003**, *19*, 341.
(8) Sullivan, R. C.; Thornberry, T.; Abbatt, J. P. D. *Atmos. Chem. Phys.* **2004**, *4*, 1301.
(9) Michel, A. E.; Usher, C. R.; Grassian, V. H. *Geophys. Res. Lett.* **2002**, *29*, 10.1029/2002GL014896.
(10) Michel, A. E.; Usher, C. R.; Grassian, V. H. *Atmos. Environ.* **2003**, *37*, 3201.
(11) Hanisch, F.; Crowley, J. N. *Atmos. Chem. Phys.* **2003**, *3*, 119.
(12) Usher, C. R.; Michel, A. E.; Stec, D.; Grassian, V. H. *Atmos. Environ.* **2003**, *37*, 5337.
(13) Che, M.; Tench, A. J. *Adv. Catal.* **1983**, *32*, 1.
(14) Katz-Tsameret, Z.; Raveh, A. *J. Vac. Sci. Technol. A* **1995**, *13*, 1121.
(15) Li, W.; Gibbs, G. V.; Oyama, S. T. *J. Am. Chem. Soc.* **1998**, *120*, 9041.
(16) Li, W.; Oyama, S. T. *J. Am. Chem. Soc.* **1998**, *120*, 9047.
(17) Cantrell, W.; Ewing, G. E. *J. Phys. Chem. B* **2001**, *105*, 5434.
(18) Estrin, D. A.; Paglieri, L.; Corongiu, G.; Clementi, E. *J. Phys. Chem.* **1996**, *100*, 8701.
(19) Dentener, F. J.; Carmichael, G. R.; Zhang, Y.; Lelieveld, J.; Crutzen, P. J. *J. Geophys. Res.* **1996**, *101*, 22869.
(20) deReus, M.; Dentener, F.; Thomas, A.; Borrmann, S.; Strom, J.; Lelieveld, J. *J. Geophys. Res.* **2000**, *105*, 15263.
(21) Alebić-Juretić, A.; Cvitaš, T.; Klasinc, L. *Chemosphere* **2000**, *41*, 667.